buildings

MDPI

Article

On-Site Monitoring and a Hybrid Prediction Method for Noise Impact on Sensitive Buildings near Urban Rail Transit

Yanmei Cao [1,*], Yefan Geng [1], Jianguo Chen [2] and Jiangchuan Ni [1]

[1] School of Civil Engineering, Beijing Jiaotong University, Beijing 100044, China; 23121007@bjtu.edu.cn (Y.G.); 23125978@bjtu.edu.cn (J.N.)
[2] Supervision Center of Engineering Quality, National Railway Administration, Beijing 100038, China; chenjianguo@nra.gov.cn
* Correspondence: ymcao@bjtu.edu.cn

Abstract

The environmental noise impact on sensitive buildings and residents, generated by urban rail transit systems, has attracted increasing attention from the public and various levels of management. Owing to the diversity of building types and the complexity of noise propagation paths, the accurate prediction of noise levels adjacent to structures through traditional experimental or empirical formula-based methods is challenging. In this paper, on-site multi-dimensional noise monitoring of the noise source affecting the sensitive buildings was first carried out, and a hybrid prediction method combining normative formulas, numerical simulations, and experimental research is proposed and validated. This approach effectively addresses the shortcomings of traditional prediction methods in terms of source strength determination, propagation path distribution, and accuracy of results. The results show that, while predicting or assessing the noise impact on sensitive buildings and interior residents, it is important to properly consider the impact of background noise (such as road traffic) as well as vibration radiation noise of bridge structures. The predicted results obtained by using this method closely match the measured results, with errors controlled within 3 dB(A). The noise prediction error in front of buildings is controlled within 2 dB(A), fully meeting the requirements for environmental noise assessment.

Keywords: noise impact; sensitive buildings; on-site monitoring; hybrid prediction method; urban rail transit

Academic Editor: Francesco Nocera

Received: 14 August 2025
Revised: 4 September 2025
Accepted: 5 September 2025
Published: 7 September 2025

Citation: Cao, Y.; Geng, Y.; Chen, J.; Ni, J. On-Site Monitoring and a Hybrid Prediction Method for Noise Impact on Sensitive Buildings near Urban Rail Transit. *Buildings* **2025**, *15*, 3227. https://doi.org/10.3390/buildings15173227

1. Introduction

Urban rail transit (URT), characterized by its large capacity, high time reliability, and efficient use of energy and land, has assumed an increasingly significant role among various transportation modes [1]. Compared to underground subway systems, elevated URT offers lower construction costs, shorter development cycles, greater flexibility, and improved visibility, which have contributed to its widespread adoption in urban areas [2]. However, urban residents living near elevated URT are adversely affected by this noise. In China, the volume of traffic noise complaints has long been at the forefront of noise complaints [3–7]. Therefore, effective prediction and control of rail traffic noise are essential, as they provide a robust scientific foundation for the development and implementation of vibration and noise reduction measures.

The noise sources from rail traffic are complex and diverse, primarily comprising wheel–rail contact noise, propulsion noise, aerodynamic noise, braking noise, and structural noise [8]. However, in urban elevated rail transit operating at speeds below 120 km/h, the

primary sources of noise are wheel–rail contact noise and bridge structure noise (Figure 1). Wheel–rail contact noise results from vibrations induced by the interaction between wheels and rails [9], which comprises rolling noise, impact noise, and squeal noise [10,11]. It is noteworthy that aerodynamic noise becomes a significant contributor at high speeds (typically above 200–250 km/h), while it is considered negligible for urban rail transit systems operating at conventional speeds. Given that the operational speed of the system under study in this paper is 68 km/h, well below the threshold where aerodynamic effects dominate, the primary noise sources are conclusively identified as wheel-rail noise and bridge structure noise. The structural noise, with low frequencies, generally below 200 Hz [12,13], is different from wheel–rail contact noise and primarily arises from vibrations in the bridge and track structures during train operation.

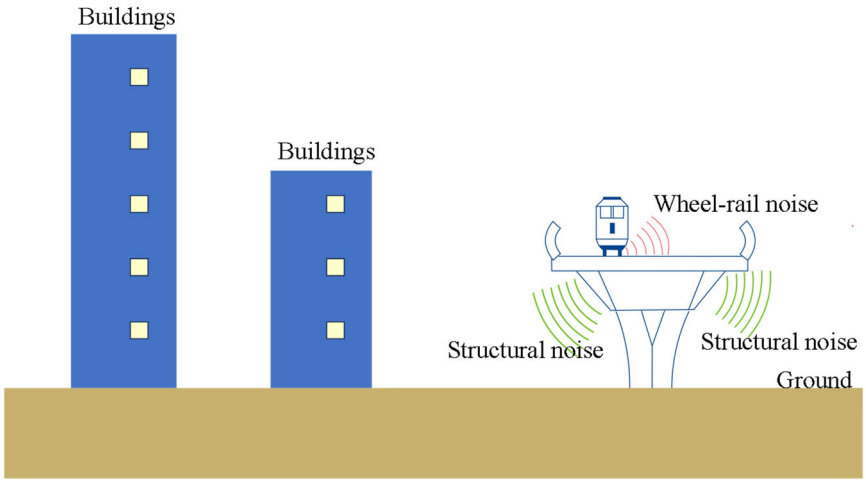

Figure 1. Primary noise sources in elevated URT elevated URT.

The primary methods for studying URT noise include field testing, theoretical analysis, and numerical simulation. He et al. [14] conducted a systematic field measurement of noise and vibration from elevated URT, considering the impact of different track structure forms on environmental noise. Shang et al. [15] measured environmental noise during rail transit train passage over the Dongshuimen Yangtze River Bridge and loop line train passing through the Changtianmen Bridge, and they found that the wheel–rail contact noise generated by trains on large-span bridges exhibited a broadband characteristic. Due to the fact that field noise testing is typically conducted in real-world environments, test conditions are subject to various factors. This can sometimes make it difficult to access certain locations or conduct tests during specific time periods, and it is also challenging to fully eliminate interference from other noise sources during field trials. Consequently, noise prediction has been predominantly investigated through theoretical analysis and numerical simulation.

Different vehicle–track coupled dynamics models have been established [16,17] and numerical simulations were used to investigate the mechanisms of wheel-rail noise generation, radiation characteristics, propagation patterns, and control technologies. Sheng et al. [18] reviewed the research progress on wheel–rail contact noise prediction models, including those for wheelset vibration and sound radiation, track structure vibration and sound radiation, and wheel–rail interaction. Based on train–track–bridge coupled vibration theory, the boundary element method (BEM) is typically employed to predict structure-borne noise from bridges and is often integrated with the finite element method (FEM) to simulate structural vibration and acoustic radiation [19]. To improve computational efficiency while keeping the 3D fidelity, Li et al. [20] proposed a two-and-a-half-dimensional (2.5D) BEM-based approach to obtain the modal acoustic transfer vectors

(MATVs) for the prediction of bridge noise. Song et al. [21,22] extended this approach to enable the prediction of noise from multi-span bridges and the investigation of both bridge and rail noise. Recently, Song et al. [23] combined the wavenumber FEM and 2D BEM for the rapid prediction of bridge noise. Yu et al. [24] developed a noise radiation model for box girder structures based on mixed finite element–statistical energy analysis theory, verified its accuracy and efficiency through experiments, and analyzed the acoustic contributions and vibration transmission characteristics. Using the pseudo-excitation method and symplectic method, Liu et al. [25] solved the dynamic response of the track system in the frequency domain and developed a hybrid prediction model combining finite element, boundary element, and statistical energy analysis. Although the theoretical analysis and numerical calculation can predict the wheel–rail contact noise and structural noise from the bridge, the time cost is very large when all kinds of field conditions need to be considered, which greatly restricts the prediction efficiency of environmental noise in engineering. In addition, the prediction methods cannot account for the complex background noise sources that exist in the actual environment.

In 2002, the European Union (EU) promulgated that Environmental Noise Assessment and Management Directive, mandating that member countries regularly produce and revise noise maps to monitor environmental noise. Subsequently, noise maps have been extensively employed as a tool for the assessment and management of urban noise. To achieve rapid prediction of environmental noise from rail transit, the "Technical Guidelines for Environmental Impact Assessment-Acoustic Environment (HJ 2.4-2021)" [26] has been released by Ministry of Ecology and Environment of China, in which empirical formulas are suggested to primarily predict environmental noise. Simultaneously, several integrated software packages have been increasingly used for rapid traffic noise prediction. For instance, the SoundPLAN software [27], released by the software designer Braunstein Berndt GmbH, can calculate the distance attenuation correction, ground absorption correction, and the superposition effect of sound reflections during sound propagation. It is commonly used for noise assessment of highway traffic. The Cadna/A software [28], developed by the German company Datakustik, can perform superposition calculations for various noise sources, accounting for multiple effects such as air absorption, distance attenuation, ground absorption, and sound reflections. It can also be used to analyze the noise reduction effects of sound barriers and to generate noise maps [29]. Furthermore, software such as Ray noise from the Belgian acoustics design company LMS, and Predictor-LimA from the Dutch Soft noise Company, are also continuously being developed and improved [30,31], and are being applied in traffic noise prediction for various scenarios. In recent years, artificial intelligence has also emerged in noise prediction. Luis et al. [32] proposed a machine learning approach for a traffic noise annoyance assessment based on noise perception, noise exposure levels, and demographics. Shashi et al. [33] investigated the utilization of artificial neural networks (ANNs) and a multiple linear regression model (MLR) for the prediction of traffic noise levels in various locations of Dhanbad city at varying intervals. Yang et al. [34] developed a rapid urban traffic noise mapping technique that leverages generative adversarial networks (GANs) as a surrogate model.

However, despite the maturity of these software packages, they exhibit significant limitations in practical engineering applications. Primarily, these software packages often rely on simplified or generic source models, which makes it difficult to accurately determine the intensity and characteristics of specific noise sources, such as the bridge-borne low-frequency structural noise prominent in elevated URT. Secondly, their prediction accuracy is highly sensitive to the input parameters relating to propagation paths and barriers. Without calibration and validation against site-specific experimental data, the results from these software packages can be unreliable, often being suitable only for rough estimations during the initial planning stage.

To overcome these limitations, this study presents a novel hybrid prediction methodology that goes beyond mere model tuning. The innovation resides in the systematic integration and cross-validation of three distinct approaches: (1) comprehensive on-site monitoring to precisely characterize complex source terms (such as wheel–rail contact, bridge structure, and background noise) and to provide validation benchmarks; (2) empirical formulas derived from national standards to ensure normative compliance and computational efficiency in basic propagation; and (3) advanced numerical simulation (Cadna/A) to manage complex propagation paths and scenarios. This framework ensures that the numerical model is rigorously calibrated and validated using multi-dimensional experimental data, thereby achieving a level of accuracy and reliability unattainable by standalone software simulations. This method provides a robust scientific foundation not only for accurate noise impact assessment but also for the effective design of noise mitigation measures.

2. Materials and Methods

The framework of the developed hybrid prediction method is illustrated in Figure 2.

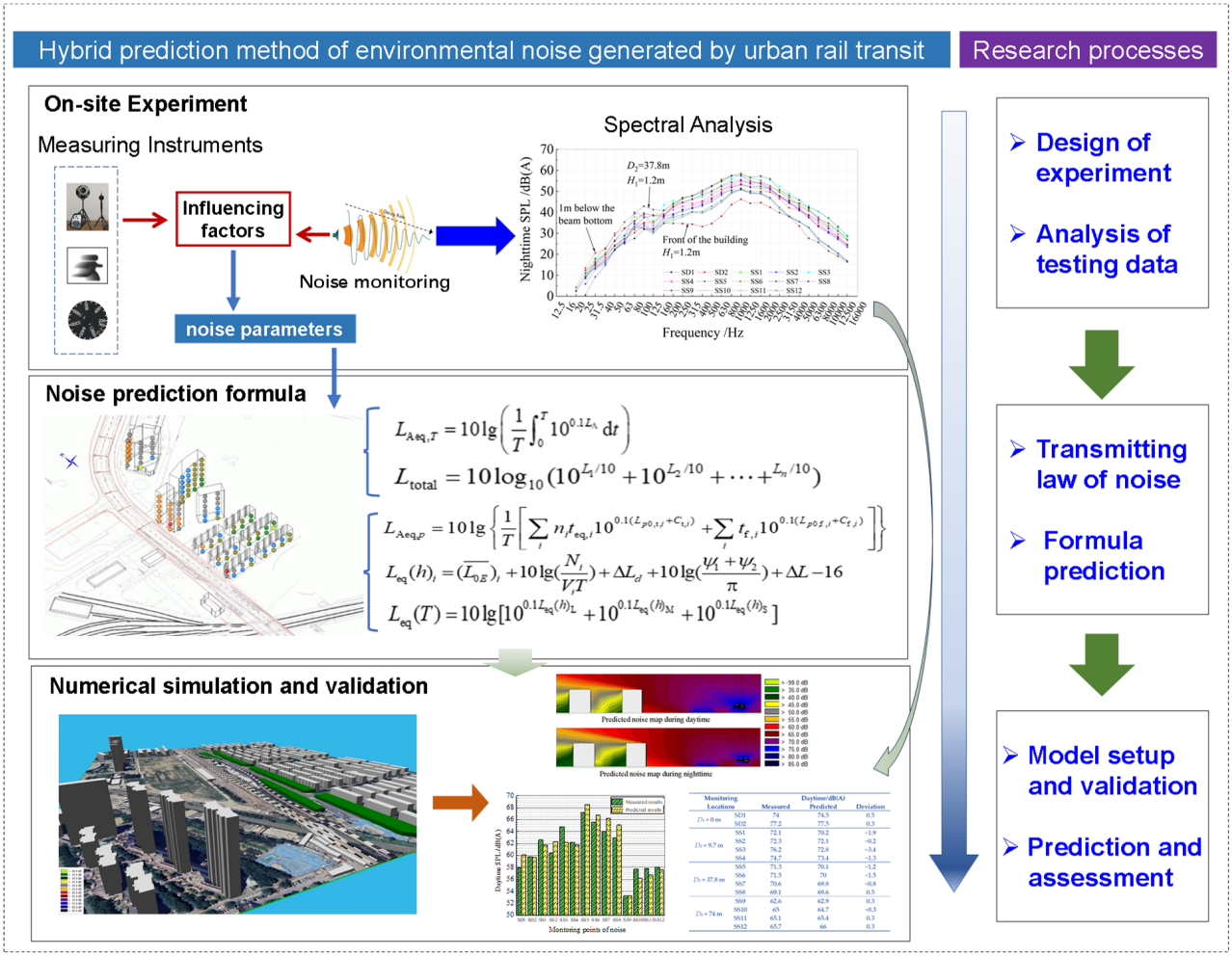

Figure 2. Hybrid prediction method framework of environmental noise.

Initially, on-site monitoring was conducted to characterize the source and propagation properties of the environmental noise along the elevated URT line. The background noise from nearby road traffic and railway traffic, bridge structural noise, and URT operation noise were identified. Subsequently, empirical formulae capable of rapidly assessing noise transmission behavior and its impact on sensitive buildings were introduced, in accordance with Chinese technical guidelines. Next, the Cadna/A, a widely used conventional outdoor ambient noise

simulation software based on empirical formulae, was employed to simulate URT noise in the chosen urban areas, and the noise mapping was achieved. However, simulation accuracy cannot be ensured if the noise source cannot be carefully determined. So, subsequently, the numerical model was further optimized and validated by dealing with on-site monitoring data as the effective input from different aspects. Finally, the hybrid prediction method was applied to assess the noise reduction effectiveness of several noise barriers.

3. On-Site Experiment

3.1. Outline of the Field Test

In order to investigate the noise characteristics from urban rail traffic and provide first-hand experimental data to support the hybrid prediction method, an environmental noise field test was conducted on an elevated bridge section of No. 13 URT line in Beijing, China. The bridge structure consists of a 3 × 25 m prestressed concrete continuous girder with a box girder cross-section, a pier height of 3.5 m, and a height difference of 5.2 m from the rail top to the ground. During peak daytime hours, approximately 22 trains operate hourly at a speed of 68 km/h, compared to roughly 9 trains per hour during nighttime operation. The building area sensitive to environmental noise is a residential neighborhood located on one side of the elevated line, primarily consisting of 6-story brick-masonry buildings (Figure 3a). In addition to urban rail noise, two significant external noise sources are present: road traffic running parallel to the tested URT line and a nearby conventional railway line. To isolate URT-generated noise from extraneous sources, all external noise was classified as background noise during testing (Figure 3b).

(**a**)

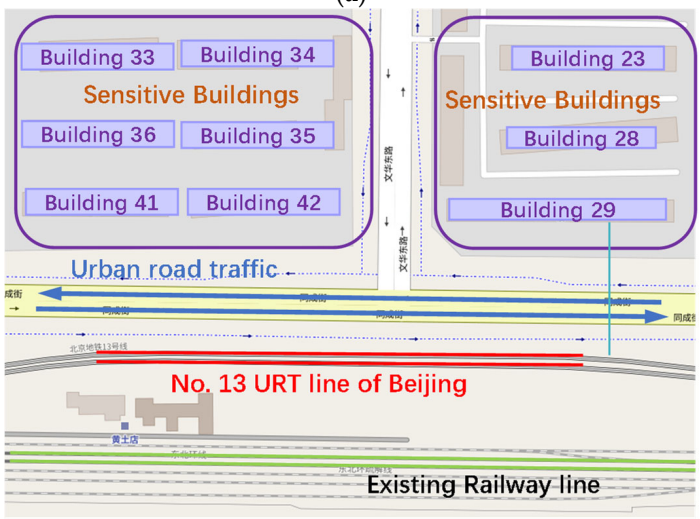

(**b**)

Figure 3. The noise sources surrounding the test site. (**a**) Elevation; (**b**) plan view.

3.2. Arrangement of Measuring Points

Based on the survey of site conditions, the elevated URT line lacks barriers or sound-proof walls on either side. Therefore, a horizontal plane parallel to the midspan of the bridge was selected as the testing cross-section, with four vertical planes designated for monitoring. Integrated circuit piezoelectric sound pressure sensors were employed as the measurement devices, with the measurement point layout illustrated in Figure 4.

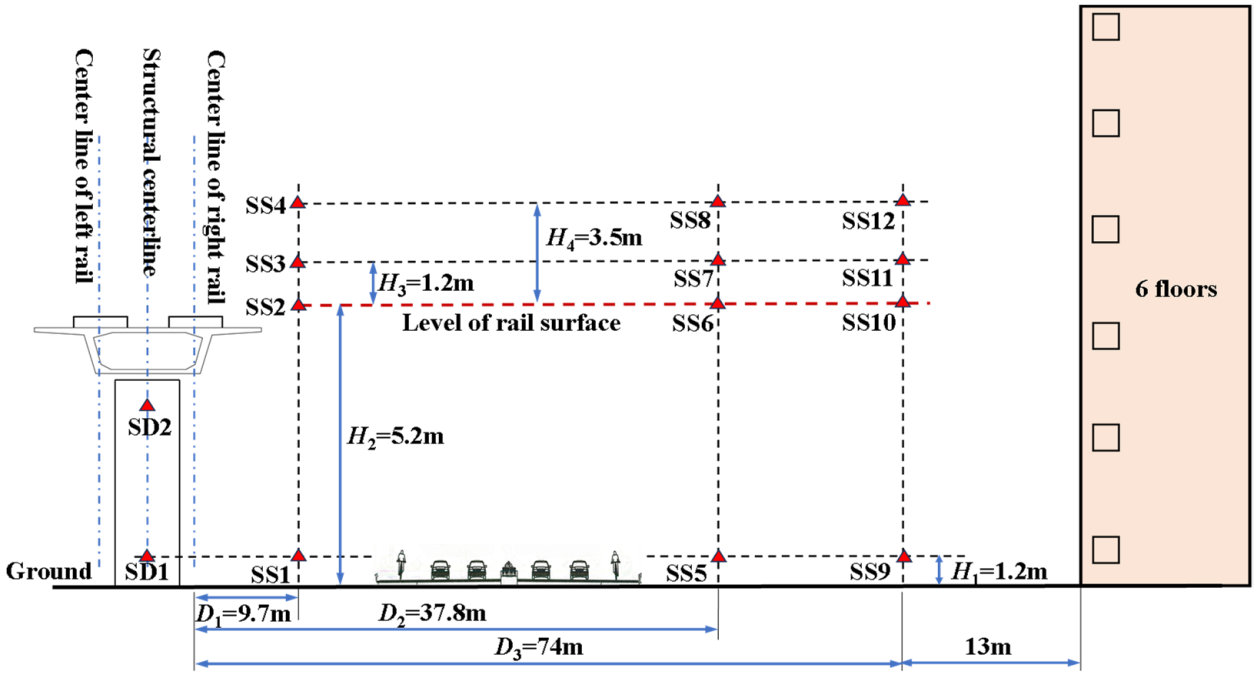

Figure 4. Layout diagram of noise measuring points.

To monitor structural noise from bridge vibration, the monitoring points SD1 (1.2 m above the ground) and SD2 (1.0 m below the beam bottom) were positioned directly beneath main beam of the bridge (D_0 = 0 m). Four points (SS1–SS4) were placed on a vertical plane, D_1 = 9.7 m horizontally from the track centerline, to measure the strength of the wheel–rail contact noise source. An additional four points (SS5–SS8) were positioned on a vertical plane, D_2 = 37.8 m horizontally from the track centerline, to monitor environmental noise along the propagation path. Four additional points (SS9–SS12) were placed 13 m in front of the building to capture noise interference around sensitive structures (D_3 = 74 m). Particularly, the monitoring points SD1, SS1, SS5, and SS9 were located H_1 = 1.2 m above ground; SS2, SS6, and SS10 were located on H_2 = 5.2 m aligned with the rail surface; SS3, SS7, and SS11 were located H_3 = 1.2 m above the rail surface; and SS4, SS8, and SS12 were located H_4 = 3.5 m above the rail surface. All monitoring point locations conform to the "Technical Guidelines for Environmental Impact Assessment—Urban Rail Transit (HJ453-2018)" issued by China's Ministry of Ecology and Environment [35]. In the technical guidelines, the measuring point of tge wheel–rail contact noise source should be arranged to be 3.5 m (when the bridge has no baffle plates on either side) or 5.0 m (when the bridge has baffle plates on both sides) above the rail surface in the vertical plane of D = 7.5 m. In this test, because there was not enough testing space at D = 7.5 m, the measuring position extended to 9.7 m from the track centerline. Moreover, due to there being no baffle plates on the bridge, the SS4 measuring point can reflect the intensity of wheel–rail contact noise.

Several field test photographs are presented in Figure 5. Sound pressure sensors continuously recorded noise signals from 16:00 to 24:00, with the period from 16:00 to 22:00 designated as daytime and 22:00–23:00 as nighttime.

(**a**) (**b**) (**c**) (**d**)

Figure 5. Field monitoring points of noise. (**a**) D_0 = 0 m; (**b**) D_1 = 9.7 m; (**c**) D_2 = 37.8 m; (**d**) D_3 = 74 m.

3.3. Analysis of Measurement Results

According to the "Technical guidelines for noise impact assessment" [26], the equivalent continuous A-weighted sound pressure level is adopted as an indicator to assess the influence level of environmental noise, which can be calculated by the following formula:

$$L_{\mathrm{Aeq},T} = 10\lg\left(\frac{1}{T}\int_0^T 10^{0.1L_{\mathrm{A}}}\mathrm{d}t\right) \quad (1)$$

where $L_{\mathrm{Aeq},T}$ is the equivalent continuous A-weighted sound pressure level (SPL) with the unit dB(A); L_{A} is instantaneous A-weighted SPL (dB(A)); and T represents the specified measurement time period (s).

3.3.1. Characteristics of Background Noise

As mentioned previously, background noise in this study refers to that generated by all sources other than URT trains, including surrounding urban road traffic, conventional railway operations, and general life activities. To evaluate the magnitude of background noise, 20 min measurement data from both daytime and nighttime periods were selected to calculate A-weighted sound pressure levels.

Table 1 presents the background noise at different measuring points, while Figure 6a compares the background noise across various vertical test planes.

Table 1. The background noise level at different measuring points.

Monitoring Locations		Background Noise Level/dB(A)		
		Day	Night	Day–Night
D_0 = 0 m	SD1 (H_1 = 1.2 m)	57.9	59.5	−1.6
	SD2 (1 m beneath beam bottom)	59.8	60.8	−1
D_1 = 9.7 m	SS1 (H_1 = 1.2 m)	62.6	62.9	−0.3
	SS2 (H_2 = 5.2 m)	60.4	60.4	0
	SS3 (H_3 = 1.2 m)	64.8	64.9	−0.1
	SS4 (H_4 = 3.5 m)	62.2	62.1	0.1
D_2 = 37.8 m	SS5 (H_1 = 1.2 m)	67.2	65.6	1.6
	SS6 (H_2 = 5.2 m)	65.6	65.1	0.5
	SS7 (H_3 = 1.2 m)	64	64.1	−0.1
	SS8 (H_4 = 3.5 m)	63	62.7	0.3
D_3 = 74 m (13 m in front of the building)	SS9 (H_1 = 1.2 m)	53.2	52.7	0.5
	SS10 (H_2 = 5.2 m)	57.7	57.1	0.6
	SS11 (H_3 = 1.2 m)	57.8	57.2	0.6
	SS12 (H_4 = 3.5 m)	58.1	57.5	0.6

It is evident that the background noise ranges from 53.2 dB(A) to 67.2 dB(A) during the daytime and from 52.7 dB(A) to 65.6 dB(A) at night. Evidently, the test site was already influenced by surrounding road and railway traffic, even in the absence of urban rail traffic. At the bottom of the beam, the background noise at night is approximately 1 dB(A) higher than that during the daytime, primarily due to the presence of workers on the rail transit

line on the test day, which led to interference from construction noise at night. Along the propagation path, the background noise during the daytime and nighttime is nearly identical; in front of the sensitive building, the background noise at night is approximately 1 dB(A) lower than during the daytime. Due to the close proximity of measuring points SS5-SS8 (D_2 = 37.8 m) to road traffic, the highest background noise levels were recorded at this vertical plane. In front of the sensitive building, the background noise at a height of 1.2 m above the ground is significantly lower than that near the elevated URT line. However, the background noises at the level of the rail surface, 1.2 m above the rail surface, and 3.5 m above the rail surface are nearly identical.

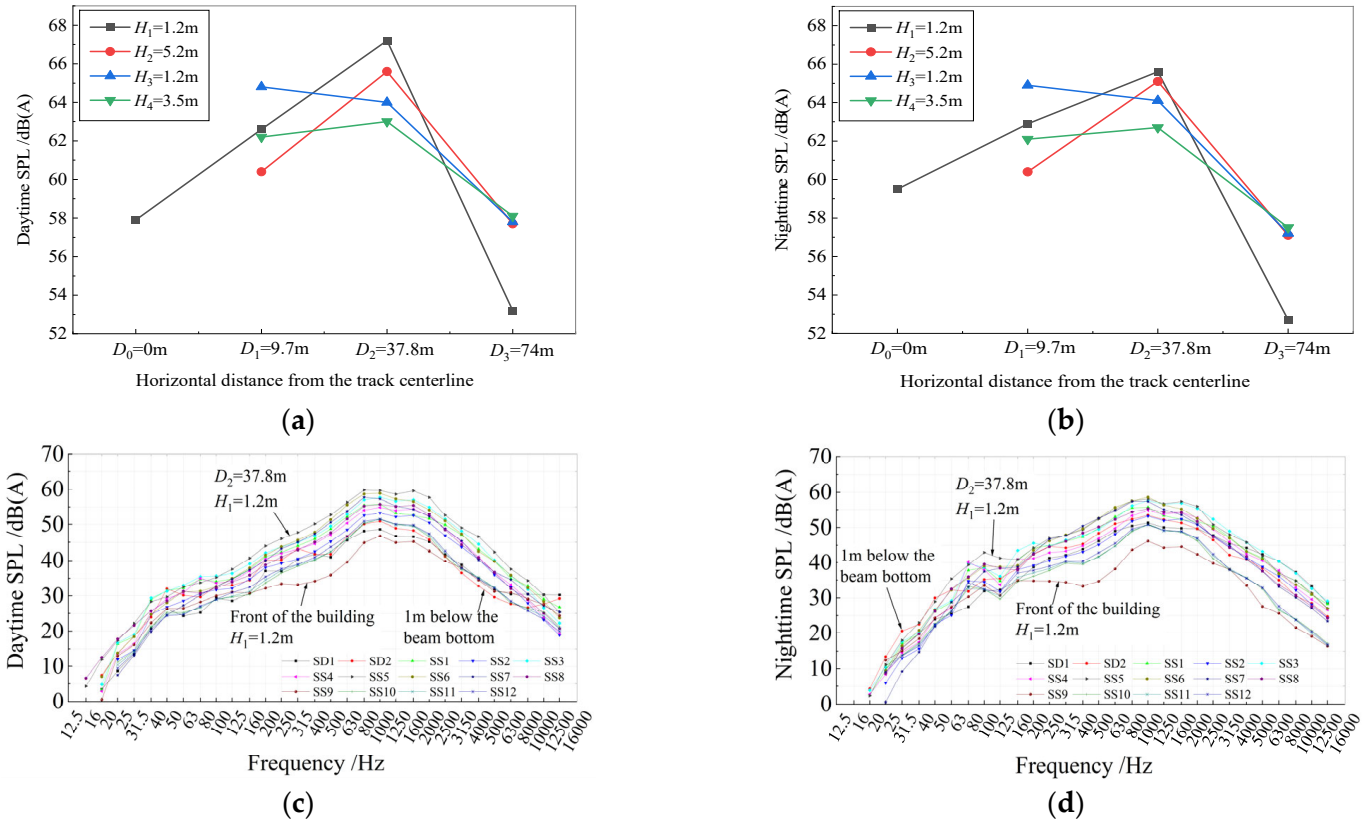

Figure 6. Magnitude and spectra of background noise. (**a**) daytime SPL; (**b**) nighttime SPL; (**c**) daytime 1/3 octave spectra; (**d**) nighttime 1/3 octave spectra.

Figure 6b presents the 1/3 octave curve of background noise for all measuring points. It is evident that the dominant frequency band of background noise during daytime at the site ranges from 630 Hz to 2000 Hz, while the dominant frequency band during nighttime spans from 630 Hz to 2500 Hz. The background noise at 1.2 m above the ground in front of building is also the lowest.

3.3.2. Characteristics of Total URT Noise

Due to the difficulty in eliminating background noise interference, the measured URT noise represents a composite environmental signal resulting from both urban rail traffic and background sources. In order to find out the characteristics of environmental noise, measurement data from peak hours (17:00–18:00 and 22:00–23:00) are used to calculate the equivalent continuous A-weighted SPL by Equation (1). Table 2 presents the measured noise levels at various measuring points during the daytime and nighttime. Figure 7 compares the URT noise across different vertical measuring planes. Daytime noise levels were found to range from 62.6 dB(A) to 77.2 dB(A), whereas nighttime levels ranged from

58.5 dB(A) to 73 dB(A). This reduction during nighttime hours is potentially attributable to variations in URT traffic flow.

Table 2. Measured urban rail traffic noise levels.

Monitoring Locations		URT Noise Level/dB(A)		
		Day	Night	Day–Night
D_1 = 0 m	SD1 (H_1 = 1.2 m)	74	70.2	3.8
	SD2 (1 m beneath beam bottom)	77.2	73	4.2
D_2 = 9.7 m	SS1 (H_1 = 1.2 m)	72.1	70.7	1.4
	SS2 (H_2 = 5.2 m)	72.3	71.2	1.1
	SS3 (H_3 = 1.2 m)	76.2	75.2	1
	SS4 (H_4 = 3.5 m)	74.7	73.5	1.2
D_3 = 37.8 m	SS5 (H_1 = 1.2 m)	71.3	68.8	2.5
	SS6 (H_2 = 5.2 m)	71.5	68.8	2.7
	SS7 (H_3 = 1.2 m)	70.6	67.9	2.7
	SS8 (H_4 = 3.5 m)	69.1	66.3	2.8
D_4 = 74 m (13 m in front of the building)	SS9 (H_1 = 1.2 m)	62.6	58.5	4.1
	SS10 (H_2 = 5.2 m)	65	61.6	3.4
	SS11 (H_3 = 1.2 m)	65.1	61.7	3.4
	SS12 (H_4 = 3.5 m)	65.7	62	3.7

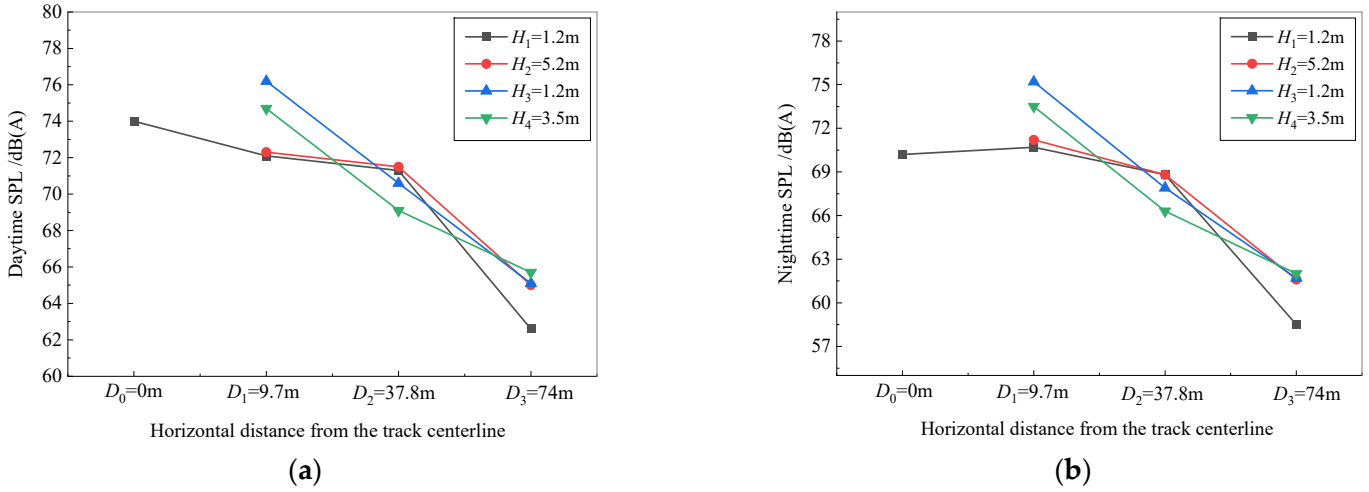

Figure 7. Environmental noise sound pressure levels caused by urban rail transit. (**a**) Daytime; (**b**) nighttime.

As shown in Figure 7, the URT noise levels gradually decrease with the horizontal distance, consistent with the physical principle of attenuation over distance. At the horizontal distance D_1 = 9.7 m from the track centerline, wheel–track contact noise was found to be reflected from the points of SS2 (H_2 = 5.2 m, aligned with the rail surface), SS3 (H_3 = 1.2 m above the rail surface), and SS4 (H_3 = 3.5 m above the rail surface). Obviously, the wheel–track contact noise of SS2 is the lowest, but that of SS3 is the greatest. Consequently, SS4 is recommended as the optimal measurement position according to technical guidelines. A comparative analysis of background noise and equivalent noise during URT operation is presented in Figure 8.

As shown in Figure 8: (1) Measured URT noise levels during operation generally exceeded background noise levels, primarily due to the superposition of multiple noise sources including background noise, bridge structure noise, and other contributing factors. (2) As the distance of the measurement point from the sound source increases, both background noise and URT noise exhibit a decreasing trend. However, the influence of background noise diminishes with increasing distance from the source, suggesting that background noise is mainly caused by road traffic adjacent to the rail transit line. (3) On the same vertical plane at the same horizontal distance, both background noise and URT noise increase with test height. However, the variation range of measured background noise is smaller, while the variation range of measured URT noise is larger. This indicates

that equivalent SPLs during URT operation are influenced by numerous variables, thereby increasing the complexity of environmental noise prediction.

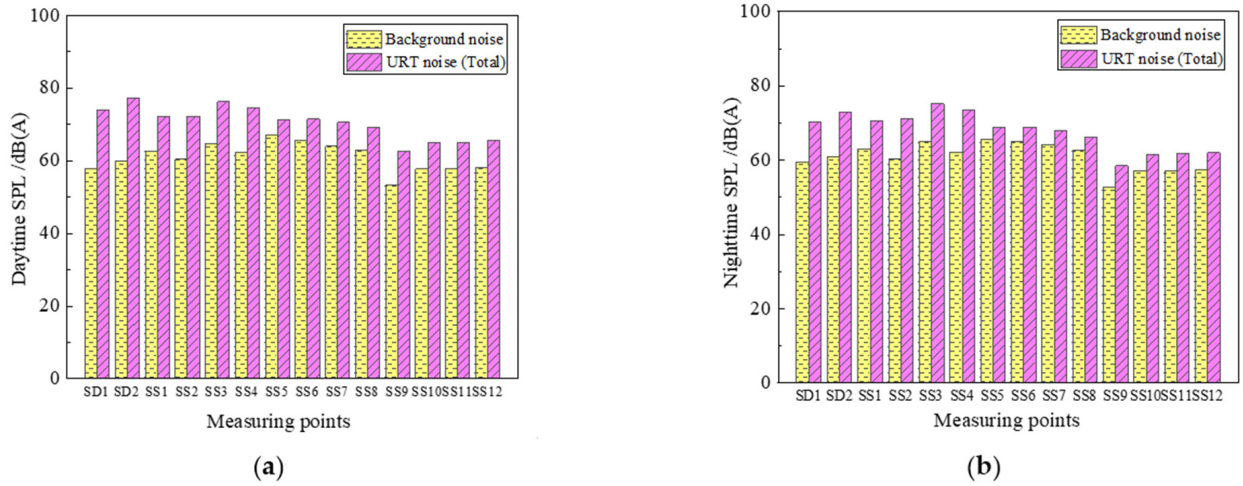

Figure 8. Comparison between background noise and operational noise levels. (**a**) Daytime; (**b**) nighttime.

Figure 9 shows the 1/3 octave band curves of the equivalent sound pressure level during the operation of URT. It can be observed that frequency peaks appear in two ranges, 50–200 Hz and 500–1000 Hz, which is different from the background noise. In the low-frequency range below 200 Hz, the noise value is highest at the position of 1 m below the bridge beam. This accurately reflects that the low-frequency noise is primarily caused by radiation noise resulting from the bridge structure's vibration induced by the URT train operation. In contrast, environmental noise above 500 Hz is mainly caused by wheel–rail contact noise and background noise.

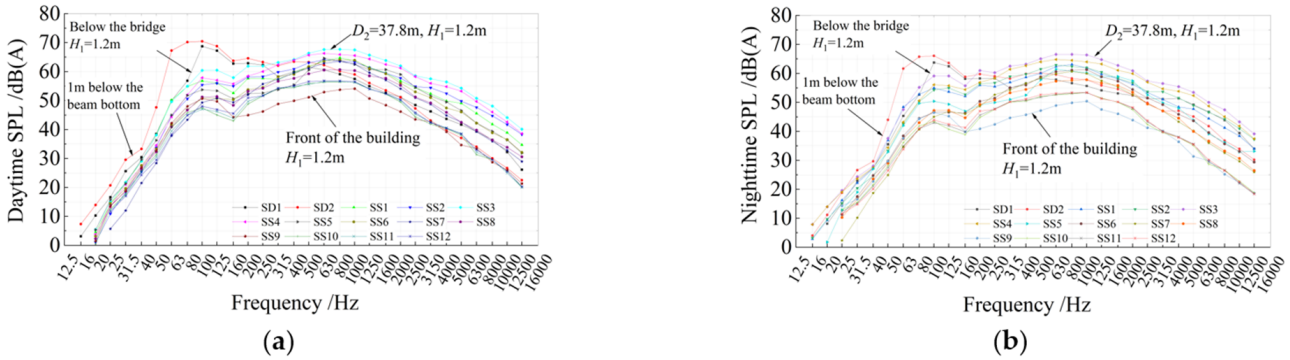

Figure 9. One-third octave spectra of environmental noise. (**a**) Daytime; (**b**) nighttime.

3.3.3. Effect of Bridge Structure Noise

Since bridge structure noise is primarily low-frequency noise below 200 Hz, the A-weighting calculation method often significantly attenuates low frequencies [36]. To further investigate the impact of secondary bridge structure noise on environmental noise during URT operation, results evaluated using unweighted SPLs (take daytime as an example) are shown in Figure 10. Environmental noise in front of sensitive buildings exhibits distinct peaks within the 50–160 Hz range, corresponding precisely to the dominant frequency band of bridge structure noise. This further demonstrates that the influence of secondary bridge structure noise must be considered in the prediction model of environmental noise caused by URT.

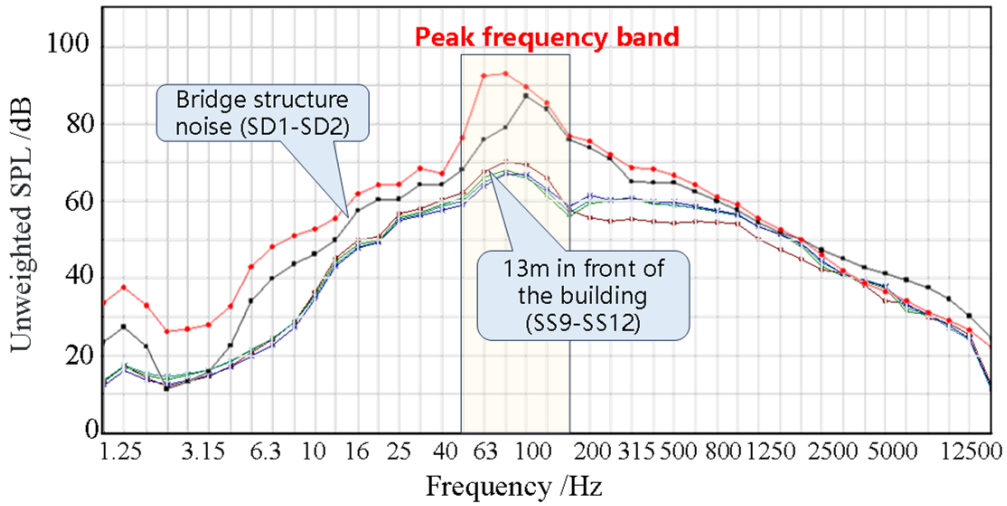

Figure 10. Unweighted sound pressure level spectra of bridge structure noise induced by elevated URT.

4. Hybrid Prediction Method and Its Validation

According to "Environmental Quality Standard for Noise (GB3096-2008)" [37], when evaluating the noise impact caused by URT by comparison with the standard limits, the measurement point should be 1 m away from the wall or window of a noise-sensitive building's exterior. However, field measurements are often constrained by limited access to noise-sensitive areas, making the placement of measurement points at the required 1 m distance from building facades impractical. Therefore, further methods are needed to accurately and efficiently predict the noise impact at 1 m in front of the sensitive building. A hybrid prediction method integrating field measurements, standardized formulas, and computational simulation is therefore proposed.

4.1. Empirical Prediction Formula of Noise Propagation

Because multiple noise sources may exist in actual environments, the "Technical Guidelines for Environmental Impact Assessment—Acoustic Environment (HJ 2.4-2021)" [26] explicitly states that the total equivalent SPL at a noise-sensitive target needs to be calculated by the superposition principle

$$L_{\text{total}} = 10\log_{10}(10^{L_1/10} + 10^{L_2/10} + \cdots + ^{L_n/10}) \quad (2)$$

where L_{total} is the total equivalent SPL (dB(A)); and L_1, L_2, …, L_n are the equivalent SPLs caused by various noise sources (dB(A)).

4.1.1. Noise Caused by URT

The noise affecting a sensitive building due to the operation of URT can be calculated by

$$L_{\text{Aeq},p} = 10\text{lg}\left\{\frac{1}{T}\left[\sum_i n_i t_{\text{eq},i} 10^{0.1(L_{p0,\text{t},i}+C_{\text{t},i})} + \sum_i t_{\text{f},i} 10^{0.1(L_{p0,\text{f},i}+C_{\text{f},i})}\right]\right\} \quad (3)$$

where T is the prescribed evaluation time (unit: s), n_i and $t_{\text{eq},i}$ are, respectively, the number and the equivalent passing time of the i-th train during T; $t_{\text{f},i}$ is the action time of fixed sound source; $L_{p0,\text{t},i}$ and $C_{\text{t},i}$ are, respectively, the intensity and correction term of the noise radiation source from the i-th train (unit: dB); $L_{p0,\text{f},i}$ and $C_{\text{f},i}$, are respectively, the intensity and correction term of the fixed sound source, which can be weighted according SPL in the time or frequency domain (unit: dB).

The equivalent time $t_{\text{eq},i}$ of the train is related to the length of the train and the running speed, and the relationship formula can be written as [26]

$$t_{\mathrm{eq},i} = \frac{l_i}{v_i} \cdot \frac{\pi}{2\arctan(\frac{l_i}{2d}) + \frac{4dl_i}{4d^2+l_i^2}} \tag{4}$$

where l_i and v_i are, respectively, the length and running speed of the i-th train, and d is the distance from the noise predicted point to the line source.

The correction terms $C_{\mathrm{t},i}$ and $C_{\mathrm{f},i}$ need to consider the influence of many factors as the following formulae:

$$C_{\mathrm{t},i} = C_{\mathrm{t},v,i} + C_{\mathrm{t},\theta} + C_{\mathrm{t},t} - A_{\mathrm{t,div}} - A_{\mathrm{atm}} - A_{\mathrm{gr}} - A_{\mathrm{bar}} - A_{\mathrm{hous}} + C_{\mathrm{hous}} + C_w \tag{5}$$

$$C_{\mathrm{f},i} = C_{\mathrm{f},\theta} - A_{\mathrm{div}} - A_{\mathrm{atm}} - A_{\mathrm{gr}} - A_{\mathrm{bar}} - A_{\mathrm{hous}} \tag{6}$$

where $C_{\mathrm{t},v,i}$ is the correction term corresponding to train speed; $C_{\mathrm{t},\theta}$ and $C_{\mathrm{f},\theta}$ are the vertical directivity correction of URT noise and fixed sound source, respectively; $C_{\mathrm{t},t}$ is the correction term corresponding to the influence of URT line type and track structure on noise, which can be determined by analogy test data, standard methods, or related data; A represents the noise attenuation in the propagation process, followed by noise geometric divergence loss (A_{div}), atmospheric absorption attenuation (A_{atm}), noise attenuation caused by ground effect (A_{gr}), insertion loss of sound barrier (A_{bar}), and attenuation caused by building group (A_{hous}); C_{hous} is the reflection correction caused by buildings on both sides; and C_w is the frequency weighting correction. The specific values of the above physical quantities can be seen in Reference [26].

4.1.2. Noise Caused by Road Traffic

The noise caused by road traffic is different from that caused by URT because the types of vehicles vary on the road continuously. Therefore, the noise caused by road traffic flow at the prediction point is calculated using another formula

$$L_{\mathrm{eq}}(T) = 10\mathrm{lg}[10^{0.1L_{\mathrm{eq}}(h)_{\mathrm{L}}} + 10^{0.1L_{\mathrm{eq}}(h)_{\mathrm{M}}} + 10^{0.1L_{\mathrm{eq}}(h)_{\mathrm{S}}}] \tag{7}$$

where $L_{\mathrm{eq}}(T)$ is the equivalent SPL caused by the total road traffic flow; and $L_{\mathrm{eq}}(h)_{\mathrm{L}}$, $L_{\mathrm{eq}}(h)_{\mathrm{M}}$ and $L_{\mathrm{eq}}(h)_{\mathrm{S}}$ are the equivalent SPL caused by large, medium and small cars, respectively, which can be calculated by the following formula

$$L_{\mathrm{eq}}(h)_i = (\overline{L_{0E}})_i + 10\mathrm{lg}(\frac{N_i}{V_i T}) + \Delta L_d + 10\mathrm{lg}(\frac{\psi_1 + \psi_2}{\pi}) + \Delta L - 16 \tag{8}$$

where $(\overline{L_{0E}})_i$ is the average A-weighted SPL generated at a horizontal distance of 7.5 m from the center line of the road when the i-th type of vehicle is traveling at vehicle speed V_i; N_i is the average hourly traffic flow of each type of vehicle passing through a predicted point during daytime or nighttime; T is the prescribed evaluation time; ΔL_d is the distance attenuation, $\Delta L_d = 10\mathrm{lg}(7.5/r)$ when the hourly traffic flow ≥ 300/hour, and $\Delta L_d = 15\mathrm{lg}(7.5/r)$ when the hourly traffic flow ≤ 300/hour, where r is the distance from the lane centerline to the predicted point (>7.5 m); and ψ_1 and ψ_2 are the angles between the predicted point and both ends of the road with a finite length (unit: rad).

The correction ΔL caused by other factors can be calculated as follows:

$$\Delta L = \Delta L_1 - \Delta L_2 + \Delta L_3 \tag{9}$$

where ΔL_1 is the correction term corresponding to the type of road; $\Delta L_1 = \Delta L_{\mathrm{slope}} + \Delta L_{\mathrm{road}}$, $\Delta L_{\mathrm{slope}}$ is the correction term for the horizontal road slope; ΔL_{road} is the correction for the road surface; ΔL_2 is the path attenuation caused by sound wave propagation; ΔL_3 is the correction term for sound reflection, and so forth. The specific values of the above physical quantities can be seen in Reference [26].

4.2. Numerical Simulation of Environmental Noise

To ensure accurate and reliable determination of environmental noise levels, the software Cadna/A (Version 2023, Datakustik GmbH, Gilching, Germany) was employed for computational analysis. Cadna/A represents an advanced environmental noise prediction tool featuring analysis modules fully compliant with China's "Technical Guidelines for Environmental Impact Assessment—Acoustic Environment" (HJ/T 2.4-2021) [26]. It not only adheres to the prediction formulas outlined in Section 4.1, but also allows for the simulation of noise sources by defining various input parameters.

4.2.1. Establishment Procedure for Noise Source–Path–Building Numerical Model

Accurate environmental noise prediction requires the construction of an environmental noise analysis model that incorporates noise sources, propagation paths, and sensitive buildings. During model establishment, detailed geographic information from satellite maps enables precise determination of spatial relationships between noise sources, buildings, terrain, and vegetation. Therefore, this study uses regional satellite maps as the base layout for the environmental noise model, enhancing modeling efficiency and prediction accuracy. However, it is important to note that satellite maps do not directly provide spatial information such as building heights, bridge heights, and tunnel depths. In such cases, on-site surveys and relevant design documentation must be consulted to accurately input parameters into the environmental noise model.

Initially, the design drawings and associated data of the rail transit line were obtained from existing CAD files, which include, but are not limited to, the track layout, URT station structure, and height information of surrounding buildings. Following import of CAD files into Cadna/A, various noise sources—including background noise, wheel–rail contact noise, and bridge structural radiation noise—were parameterized. Simultaneously, two calculation cases corresponding to background noise and equivalent noise were configured, enabling the environmental noise model to accurately reflect real-world conditions.

4.2.2. Determination of Model Dimensions

When building the model, all potential noise sources that could affect sensitive receivers or buildings must be included, along with those factors contributing to noise attenuation, such as building clusters, green belts, and topography. Therefore, the model boundary must extend beyond the noise-affected area to ensure simulation accuracy. In addition, the actual affected area should be determined by referencing the approximate actual monitoring data and the noise limits specified in the standards. Ultimately, the lateral dimension of the model should at least extend two vehicle lengths on each side of the track, while the longitudinal dimension should encompass sensitive buildings and the nearest residential areas affected by noise on the southern side of the rail transit line.

As an example, the established environmental noise model based on the actual engineering project of Beijing Subway Line 13 described in Section 3, is presented in Figure 11. The model length and width are 1300 m and 900 m, respectively. The sound sources, propagation paths, and sensitive buildings in the model show close alignment with the actual environment depicted in Figure 3.

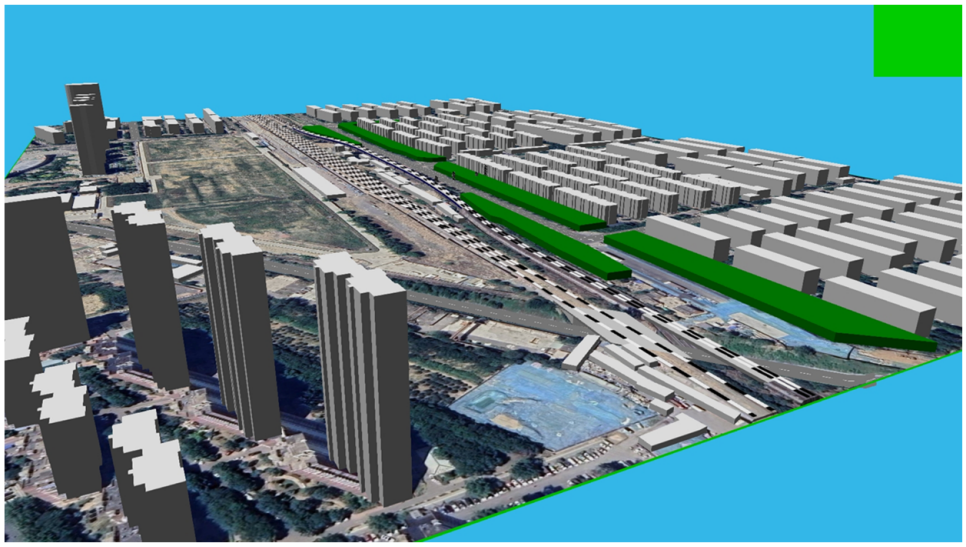

Figure 11. Three-dimensional view of noise source–path–building numerical model.

4.2.3. Simulations of Different Noise Sources

As indicated in Equations (2)–(9), noise levels can be predicted based on various sound source types and their propagation characteristics. Once the SPLs at the position of each noise source are determined, the corresponding SPLs in front of sensitive buildings can be obtained by sequentially overlaying correction terms related to influencing variables of noise propagation. Therefore, the accurate determination of noise source levels is very crucial for ensuring prediction accuracy. Take the actual engineering project of Beijing Subway Line 13 described in Section 3 as an example, the simulations of different noise sources are described as follows.

(1) Simulation of background noise source

The primary sources of background noise include road traffic and conventional railway noise near sensitive buildings. In modeling road traffic noise, parameters such as road width, hourly traffic volume, heavy vehicle proportion, vehicle speed, and road gradient are input based on actual monitoring data, alongside the selection of pavement materials, to generate an uncorrected road noise model. The modeling of conventional railway noise follows a similar approach to wheel–rail contact noise, which will be discussed later. The application of these background noise sources is illustrated in Figure 12a.

(2) Simulation of wheel–track contact noise source

Wheel–rail contact noise was simulated using a line source model parameterized with operational and geometric data. The train operating speed for calculating the equivalent SPL was obtained through on-site monitoring, with the average speed of five trains used as the final measured value. The train composition length is obtained from the design documents. The number of trains is determined by the train speed, operating time, and train length. The train noise source is input by using the noise value measured at 3.5 m above the track surface during on-site monitoring. The track and ground elevation data are sourced from design documents and topographical maps. The length and height of the sound barriers are based on actual survey results and design documents. The model of the wheel–rail contact noise source is shown in Figure 12b.

(3) Simulation of structural radiation source of bridge

The wheel–track contact noise can be simulated by a surface sound source with a series of parameters. High-sensitivity acoustic sensors were placed directly beneath the

URT bridge to collect noise data under actual operating conditions. Accordingly, noise measurements obtained at location SD2 (Section 2) were incorporated into the model as input parameters. These data were used as surface noise sources (Figure 12c) in the environmental noise model.

It is noteworthy that the atmospheric pressure, temperature, and humidity may influence the noise propagation. In establishing the model, the atmospheric temperature, humidity, and pressure have been set to be 20 °C, 50%, and 101.325 kPa, respectively. These values are particularly close to the actual atmospheric conditions on the day of the on-site measurement. Since the emphasis of the model validation is on calibrating source strengths and propagation paths, the influence of slight meteorological variations on the results for the short distances involved is deemed secondary and acceptable for the purposes of engineering assessment.

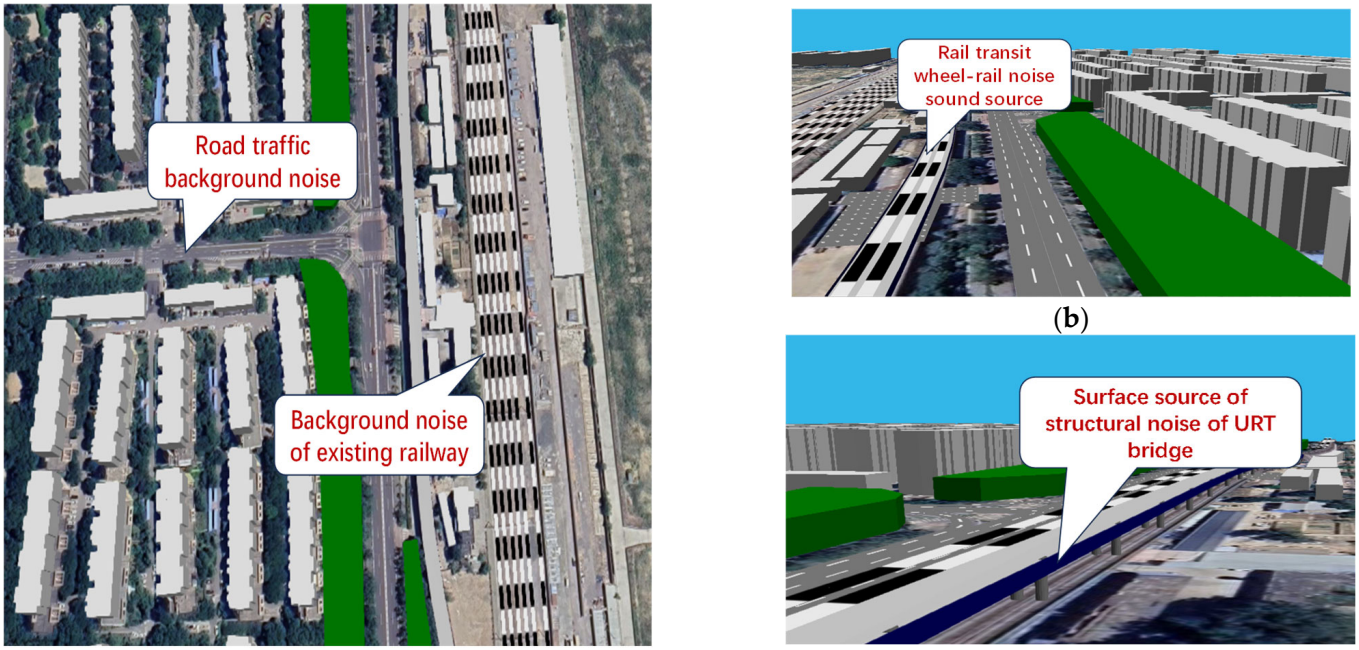

Figure 12. One-third octave spectra of environmental noise. (**a**) Background noise source; (**b**) wheel–rail contact noise source; (**c**) bridge structure noise.

4.3. Hybrid Prediction Model of Environmental Noise

Given the complexity of the existing noise sources and the density of acoustic environment protection targets, a hybrid model integrating on-site experiments, prediction formulas, and numerical simulations was developed to achieve reliable and accurate prediction results.

Following the construction of the preliminary model, initial calculations were conducted. The model was subsequently optimized through an iterative process (Figure 13), wherein the background noise source parameters are refined by comparing them with the measured background noise data. Subsequently, information on the equivalent train trips is input to calculate the equivalent SPL. This calculated level is then compared with the actual measured equivalent data, facilitating adjustments to the train parameters in the model to improve prediction accuracy. The accuracy requirement for this study was set at ±3 dB(A), in accordance with Section 7.3.2 of the HJ/T 2.4-2021 [26] guidelines.

Once the model optimization is complete, predictions can be made for additional receiver points along the section. Furthermore, a sound barrier model can be constructed, and its noise reduction effectiveness can be assessed by comparing data before and after the installation of the barrier. This systematic approach facilitates the development of a highly

accurate prediction model, providing robust support for analyzing and evaluating the impact of various noise sources on the environment.

To ensure the reproducibility and transparency of the numerical simulations, the key input parameters, traffic flow data, and model configuration settings used in the Cadna/A predictions are comprehensively documented in Appendix A. This includes the source strengths, ground properties, meteorological conditions, and calculation settings that were essential for achieving the accurate results presented in Section 4.4.

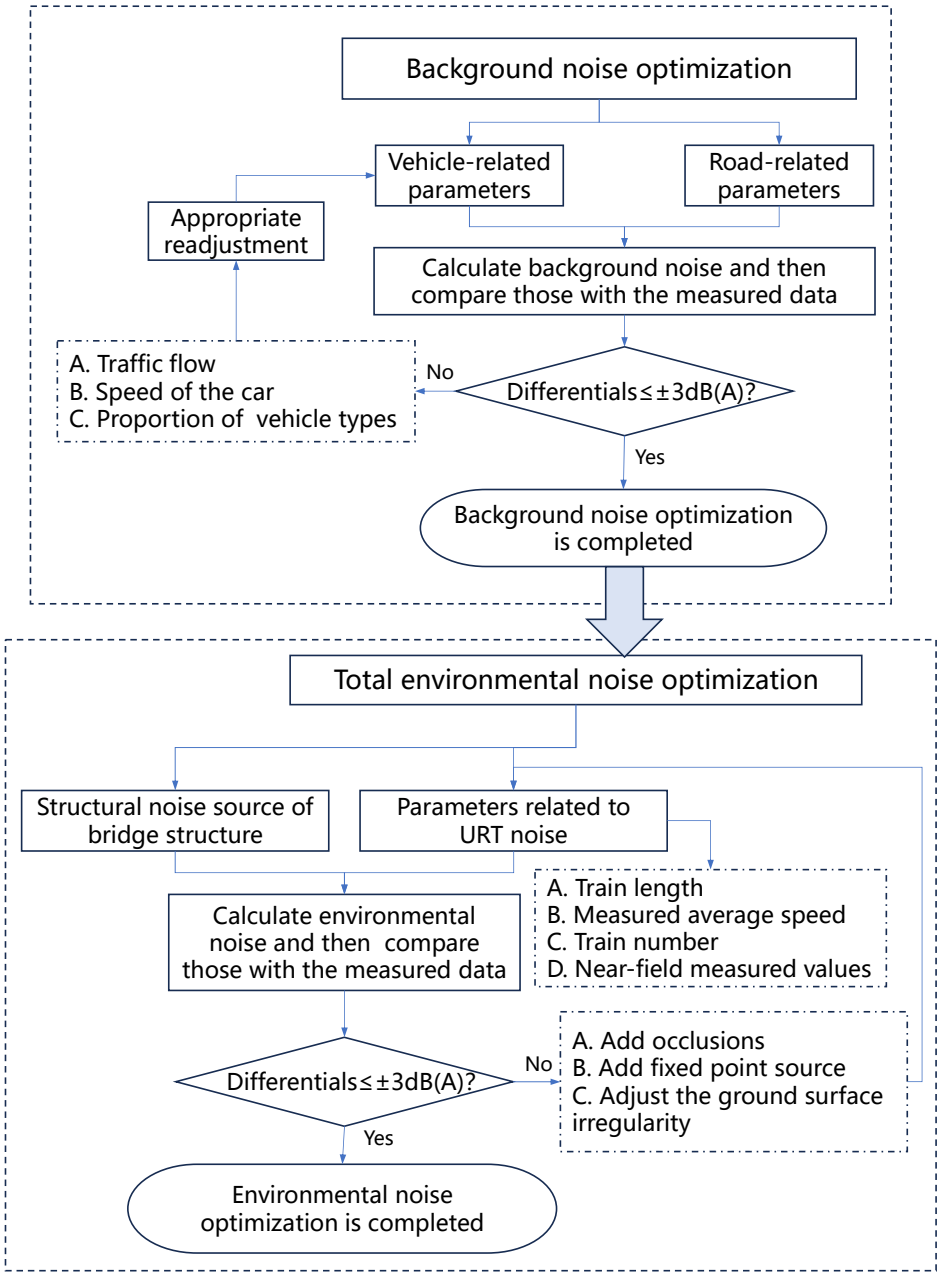

Figure 13. Process of model optimization.

4.4. Results and Verification of Hybrid Prediction Model

The hybrid prediction model is validated by comparing the numerical results with measured data obtained at various horizontal distance points in Section 3.

The first step is to validate the accuracy of background noise. Figure 14 presents a comparison of the equivalent sound pressure level between the calculated and measured background noise levels. Although the measured data is a little discrete, the actual variation

in ambient background noise is relatively stable during 20 min without the URT running. It can be found that the deviation between the predicted and measured values is minimal. During the daytime, at the monitoring point SS9 (13 m in front of the building, H_1 = 1.2 m above ground), the predicted value aligns precisely with the measured value. Due to the nighttime construction on the track during the experimental monitoring process, there was significant interference with the nighttime background noise, resulting in a slight deviation between the predicted values and the measured values. All deviations remained within ±3 dB(A), thereby satisfying the accuracy requirements.

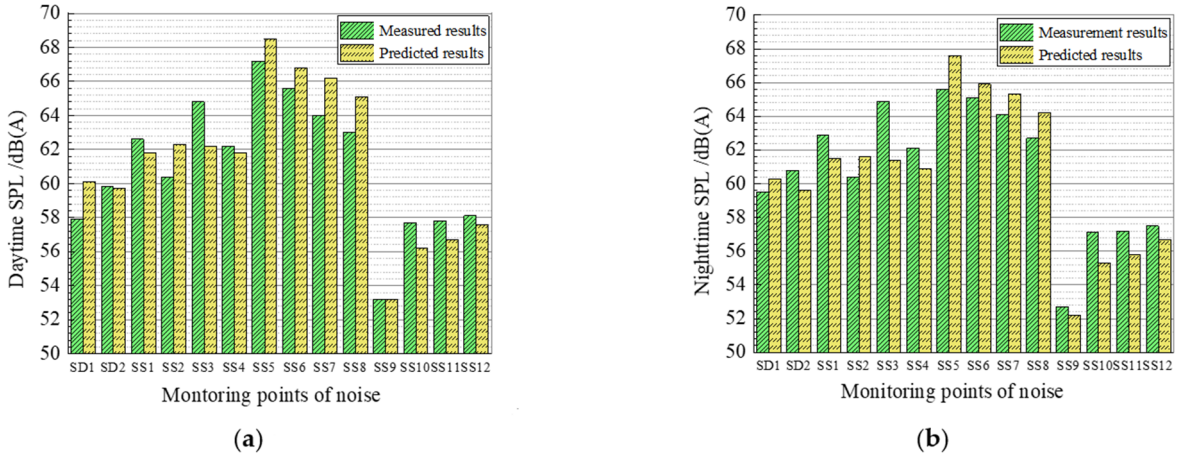

(**a**) (**b**)

Figure 14. Validation of background noise results. (**a**) Daytime; (**b**) nighttime.

The second step is to validate the accuracy of the total environmental noise levels, which are noise rating values in environmental noise evaluation. Taking the background noise source, wheel–track contact noise source, and structural radiation noise of the bridge into account, both the predicted results and the measured data are showed in Table 3.

Table 3. Validation of the predicted environmental noise levels.

Monitoring Locations		Daytime/dB(A) Measured	Daytime/dB(A) Predicted	Daytime/dB(A) Deviation	Nighttime/dB(A) Measured	Nighttime/dB(A) Predicted	Nighttime/dB(A) Deviation
D_1 = 0 m	SD1	74	74.5	0.5	70.2	70.5	0.3
	SD2	77.2	77.5	0.3	73	73.4	0.4
D_2 = 9.7 m	SS1	72.1	70.2	−1.9	70.7	66.8	−3.9
	SS2	72.3	72.1	−0.2	71.2	68.4	−2.8
	SS3	76.2	72.8	−3.4	75.2	69	−6.2
	SS4	74.7	73.4	−1.3	73.5	69.5	−4
D_3 = 37.8 m	SS5	71.3	70.1	−1.2	68.8	68.4	−0.4
	SS6	71.5	70	−1.5	68.8	67.7	−1.1
	SS7	70.6	69.8	−0.8	67.9	67.4	−0.5
	SS8	69.1	69.6	0.5	66.3	66.8	0.5
D_4 = 74 m	SS9	62.6	62.9	0.3	58.5	59.1	0.6
	SS10	65	64.7	−0.3	61.6	61.1	−0.5
	SS11	65.1	65.4	0.3	61.7	61.7	0
	SS12	65.7	66	0.3	62	62.4	0.4

The deviations presented in Table 3 represent the predicted values minus the measured values. A positive result indicates that the predicted value is higher than the measured value, while a negative result indicates the opposite. By comparing the predicted values with the measured values, it can be seen that, except for measuring point SS3 at 1.2 m above the rail surface, where the predicted value is slightly lower (the main reason being that the measuring point is close to the rail surface and is affected by additional factors), the predicted values of the other measuring points are very close to the actual results. Especially in front of the sensitive buildings, which are of great concern in noise impact assessment, the difference between the two is only 0.3 dB(A) to 0.6 dB(A). The noise impact

assessment results obtained through the proposed prediction method demonstrate high accuracy and reliability, confirming its applicability for predicting and assessing noise impact on sensitive buildings along rail transit lines.

5. Application Examples of Hybrid Prediction Method

5.1. Environmental Noise Prediction and Evaluation

The hybrid prediction method enables convenient, rapid, accurate, and efficient prediction and assessment of environmental noise impact on sensitive buildings (Figure 15). Using the sensitive buildings from the Section 3 field experiment as an example, noise levels at 1 m from all sensitive buildings were predicted for each floor height, as summarized in Table 4 (only the first row of buildings is shown).

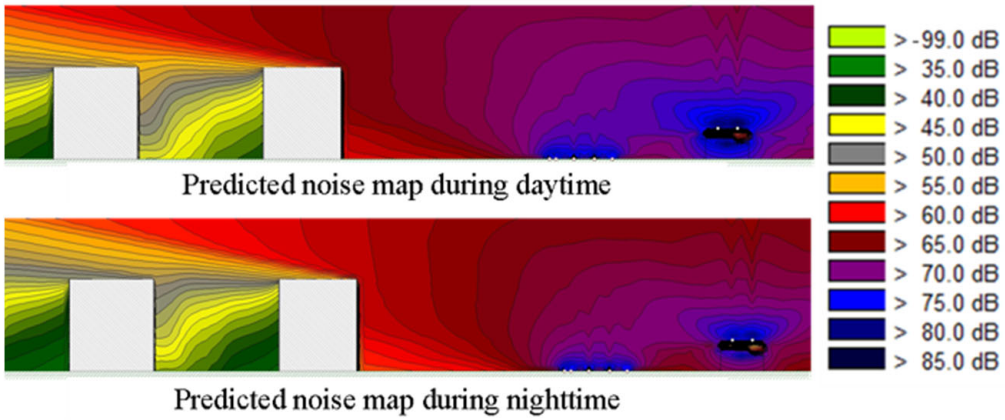

Figure 15. Prediction and evaluation of environmental noise influence.

Table 4. Predicted noise levels and exceedance situations in front of the first row of sensitive buildings.

First Row of Buildings	Predicted/dB(A)		Noise Limit/dB(A)		Exceedance/dB(A)	
Floor	Day	Night	Day	Night	Day	Night
1F	61.8	59.0	70.0	55.0	—	4.0
2F	62.7	60.0	70.0	55.0	—	5.0
3F	64.1	61.4	70.0	55.0	—	6.4
4F	64.8	62.2	70.0	55.0	—	7.2
5F	64.8	62.3	70.0	55.0	—	7.3
6F	64.8	62.4	70.0	55.0	—	7.4

Note: "—" indicates that the predicted noise level is below the stipulated limit, meaning there is no exceedance.

Since the acoustic function area near sensitive building belongs to Class 4a, the stipulated noise limits of the first row of buildings are 70 dB(A) during the daytime and 55 dB(A) during nighttime, and the noise limits of the second row of buildings are 55 dB(A) during the daytime and 45 dB(A) during nighttime [37]. Comparison between the predicted noise levels and the stipulated limits for this Class 4a acoustic function area reveals that, during URT operation, environmental noise remains within daytime standards but exceeds nighttime limits due to the combined influence of wheel–rail contact noise, background noise, and bridge structure-borne noise. Moreover, the higher the floor number, the more serious the nighttime exceedance. The implementation of noise barriers and additional noise control measures is therefore recommended for this URT section.

5.2. Noise Reduction Effect Analysis of Different Types of Sound Barriers

A sound barrier is a structure designed to mitigate the impact of traffic noise on the surrounding environment by blocking, absorbing, and reflecting sound waves. Typical barrier configurations include vertical, semi-enclosed, and fully enclosed designs. Using

the validated hybrid prediction method, the noise reduction performance of various barrier types can be quantified through comparative analysis of pre- and post-installation data.

In this analysis, the noise reduction effects of several barrier configurations were evaluated by defining their acoustic properties within the Cadna/A model. The following cases were considered: (1) Vertical barriers: Two heights were analyzed: a 3 m high barrier and a 5 m high barrier. The barriers were modeled as acoustically hard surfaces with a low absorption coefficient, primarily causing sound reflection rather than absorption. (2) Semi-enclosed barrier: A barrier that partially encloses the track with side walls and an overhead canopy. A uniform absorption coefficient of 0.5 was assigned to its interior surfaces to model its acoustic performance. (3) Fully enclosed barrier: A structure that completely encapsulates the track (a noise shed). A uniform absorption coefficient of 0.7 was assigned to its interior surfaces to model its acoustic performance.

For all barrier types, the key acoustic parameter input into the model was the absorption coefficient across relevant frequency bands, which defines the amount of sound energy absorbed by the barrier surface rather than reflected. The insertion loss (noise reduction) of each barrier type was then calculated by the software according to the international standard ISO 9613-2 [38], based on these defined properties and the geometry of the setup.

Figure 16 demonstrates significant noise reduction effects during both day and night with the application of sound barriers. The installation of a vertical sound barrier with 3 m height reduces noise levels by 3–4 dB(A). Although increasing the barrier height enhances noise reduction, the incremental improvement diminishes with greater height. The noise reduction performance between fully enclosed and semi-enclosed sound barriers shows minimal differences, the equivalent noise reduction effects are observed across most measurement points at various building floors. Barrier selection should therefore be based on comprehensive consideration of practical constraints, noise reduction efficiency, cost, esthetics, and maintenance requirements.

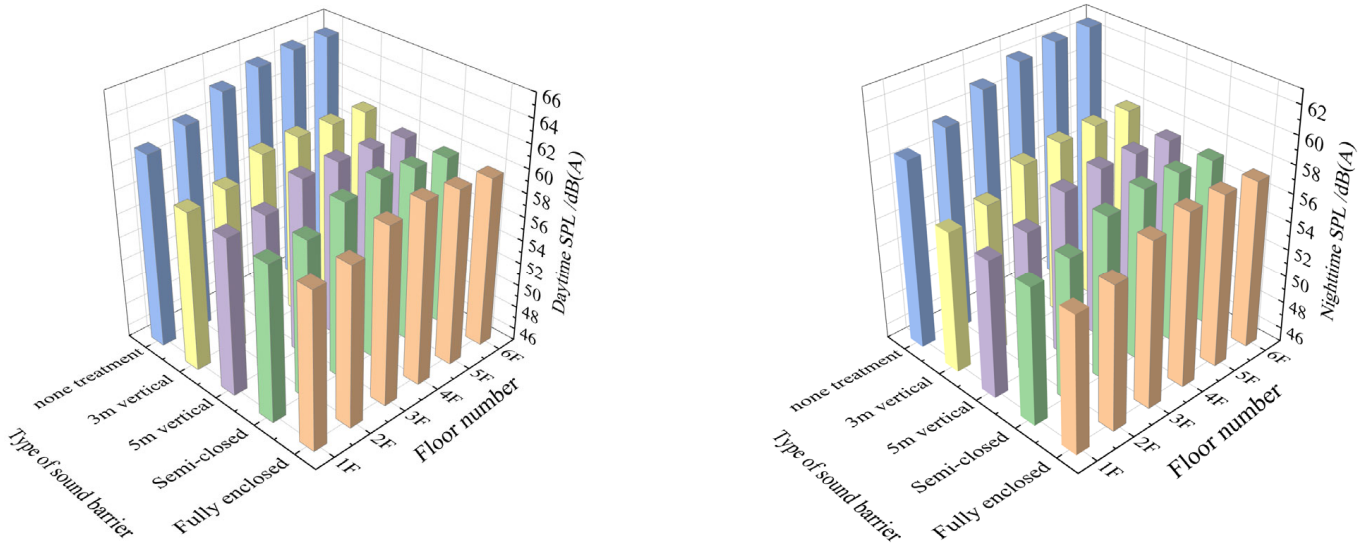

Figure 16. Calculation results of applying different sound barriers. (**a**) Daytime; (**b**) Nighttime.

The simulation results demonstrate that both semi-enclosed and fully enclosed barriers offer superior noise reduction compared to vertical barriers. Although their acoustic performance is comparable, the semi-enclosed barrier is recommended as the most favorable solution for this project. This recommendation is based on its optimal balance of high noise abatement effectiveness, lower construction and maintenance costs relative to a fully enclosed structure, and less visual intrusion on the urban landscape. The semi-enclosed

design provides a cost-effective and efficient strategy for mitigating rail transit noise impact on the surrounding sensitive buildings.

5.3. Limitations and Generalizability of the Proposed Method

The proposed hybrid method, while demonstrating high accuracy in this case study, is not without its limitations and constraints on generalizability. The following points discuss these aspects to provide a balanced view of the method's scope.

The primary limitation of this study is that its validation is based on a single case study. Although the method is theoretically applicable to various elevated urban rail transit (URT) scenarios, its predictive accuracy for lines with significantly different structural types (e.g., steel bridges or viaducts), operational conditions (e.g., higher speeds or different train types), or complex urban canyon environments needs to be further verified through additional case studies. Moreover, the method requires extensive on-site monitoring for model calibration, which could be resource-intensive for large-scale network-wide assessments.

In terms of generalizability, the framework integrating monitoring, empirical formulas, and numerical simulation is universally applicable. The key to transferring this approach lies in the accurate acquisition of site-specific parameters, particularly the characterization of dominant noise sources (both strength and spectrum). For future applications, it is recommended that a preliminary survey be conducted first to identify the key noise sources and propagation paths specific to the new site, followed by the established workflow presented in this paper for modeling and calibration. Future work will focus on developing a simplified parameter selection guide to enhance the method's efficiency and applicability for rapid preliminary assessments.

6. Conclusions

Based on the engineering example of Beijing Subway Line 13, an on-site test of rail transit environmental noise was carried out and a hybrid prediction method was proposed. The noise hybrid prediction method highly integrates on-site testing, prediction formulas, and modeling analysis with calculation software. It effectively makes up for the shortcomings of traditional single-prediction methods, and has significant advantages in the accurate simulation of various types of noise source. The main conclusions are as follows:

(1) Noise with a frequency lower than 200 Hz is primarily caused by radiation noise resulting from the vibration of the bridge structure induced by the URT train operation. In contrast, environmental noise above 500 Hz is mainly caused by wheel–rail contact noise and background noise.

(2) In actual engineering, the background noise is usually very complex due to ambient disturbances. Urban rail transit noise prediction must comprehensively account for the influence of ambient background noise and bridge vibration-induced structural radiation noise. Also, the numerical results for background noise should be validated by on-site measurement data.

(3) In order to ensure the applicability and reliability of the hybrid prediction method under different conditions, the optimization and correction of the calculation model, as well as multi-dimensional and multi-point experimental data verification of different noise sources, are necessary.

(4) The error between the predicted results and the measured results can be controlled within 3 dB(A), and the noise prediction error in front of buildings can be controlled within 2 dB(A), which fully meets the requirements for environmental noise assessment.

(5) The hybrid prediction model enables both assessment of urban rail transit noise impact on sensitive buildings and evaluation of noise reduction effectiveness for various barrier types. By adjusting and calculating the parameters of noise barriers in the model, the

noise reduction performance of various noise barriers can be intuitively displayed, providing data support and scientific basis for the design and selection of noise control measures.

Author Contributions: Conceptualization, Y.C.; methodology, Y.C. and Y.G.; software, Y.G.; validation, Y.C., Y.G., and J.C.; formal analysis, Y.C. and Y.G.; investigation, J.C. and J.N.; resources, J.C.; data curation, J.N.; writing—original draft preparation, Y.G.; writing—review and editing, Y.C.; supervision, Y.C.; project administration, Y.C.; funding acquisition, Y.C. All authors have read and agreed to the published version of the manuscript.

Funding: This research was funded by the Beijing Natural Science Foundation-Fengtai Frontier Project, grant number L241077.

Data Availability Statement: The data provided in this study could be released upon reasonable request. The authors state that all data, models, and code generated or used during this study are available from the corresponding author by request. The responsibility for scientific accuracy and content remains entirely with the authors.

Acknowledgments: We would like to thank the Beijiao Zane Rail Technology (Beijing) Co., Ltd., China for providing the on-site experimental conditions and some test applicants. We would also like to express our deep gratitude to the editors and peer reviewers for their many valuable comments.

Conflicts of Interest: The authors declare that the research was conducted in the absence of any commercial or financial relationships that could be construed as potential conflicts of interest.

Appendix A

To ensure the reproducibility of this study, this appendix provides the key input parameters and settings used in the Cadna/A numerical model, as requested by the reviewers.

Table A1. Traffic flow parameters for Beijing Metro Line 13 (tested section).

Parameter	Daytime	Nighttime	Notes
Train type	Type B (6 cars)	Type B (6 cars)	Design document
Train length	118 m	118 m	Design document
Train speed	68 km/h	68 km/h	On-site test (Section 3.1)
Traffic volume	22 trains/h	9 trains/h	On-site test (Section 3.1)

Table A2. Key input parameters in Cadna/A numerical model.

Parameter Category	Value/Setting	Notes/Source
Wheel–rail source height	3.5 m above rail top	Regulated by codes
Wheel–rail source SPL	74.7 dB(A) (Day), 73.5 dB(A) (Night)	On-site test (Table 2, line source)
Structure noise SPL from bridge	77.2 dB(A) (Day), 73.0 dB(A) (Night)	On-site test (Table 2, surface source)
Ground type	Hard (asphalt, concrete)	On site road survey
Building facades	Reflection coefficient: 0.9	Brick/concrete structures

Table A3. Calculation settings.

Setting	Value/Option	Notes
Temperature	20 °C	Common value recommended by ISO 9613-2
Humidity	50%	Common value recommended by ISO 9613-2
Atmospheric pressure	101.325 kPa	Common value recommended by ISO 9613-2
Calculation principle	Evaluation standard (HJ 2.4-2021) [26]	Selected by the users Ensure the propagation algorithm in the software is compatible with this standard
Propagation model	Defined by the adopted code	Automatically invoked by the software based on the propagation model from ISO 9613-2

References

1. Lin, D.; Nelson, J.D.; Beecroft, M.; Cui, J. An overview of recent developments in China's metro systems. *Tunn. Undergr. Space Technol. Tunn* **2021**, *111*, 103783. [CrossRef]
2. Sheng, X. A review on modelling ground vibrations generated by underground trains. *Int. J. Rail Transp.* **2019**, *7*, 241–261. [CrossRef]
3. *Annual Report on Prevention and Control of Noise Pollution in China*; Ministry of Ecology and Environment of China: Beijing, China, 2024.
4. Thompson, D.J.; Kouroussis, G.; Ntotsios, E. Modelling, simulation and evaluation of ground vibration caused by rail vehicles. *Veh. Syst. Dyn.* **2019**, *57*, 936–983. [CrossRef]
5. Qiu, Y.; Zou, C.; Wu, J.; Shen, Z.; Zhong, Z. Building vibration measurements induced by train operation on concrete floor. *Constr. Build. Mater.* **2023**, *394*, 132283. [CrossRef]
6. Hao, Y.; Qi, H.; Liu, S.; Nian, V.; Zhang, Z. Study of noise and vibration impacts to buildings due to urban rail transit and mitigation measures. *Sustainability* **2022**, *14*, 3119. [CrossRef]
7. Qiu, Y.; Zheng, B.; Jiang, B.; Jiang, S.; Zou, C. Effect of non-structural components on over-track building vibrations induced by train operations on concrete floor. *Int. J. Struct. Stab. Dyn.* **2025**, 2650180. [CrossRef]
8. Remington, P.J. Wheel\rail rolling noise I: Theoretical analysis. *J. Acoust. Soc. Am.* **1987**, *81*, 1805. [CrossRef]
9. Thompson, D.; Jones, C. A review of the modelling of wheel/rail noise generation. *J. Sound Vib.* **2000**, *231*, 519–536. [CrossRef]
10. Zea, E.; Fernandez-Grande, E.; Arteaga, I.L. Separation of rail and wheel contributions to pass-by noise with sparse regularization methods. *J. Sound Vib.* **2020**, *487*, 115627. [CrossRef]
11. Li, Q.; Alemi, M.M. Review study of main sources of noise generation at wheel-rail interaction. *J. Acoust. Soc. Am.* **2016**, *139*, 2205. [CrossRef]
12. Li, Q.; Dai, B.; Zhu, Z.; Thompson, D.J. Comparison of vibration and noise characteristics of urban rail transit bridges with box-girder and U-shaped sections. *Appl. Acoust.* **2022**, *186*, 108494. [CrossRef]
13. Gu, Y.W.; Nie, X.; Yan, A.G.; Zeng, J.H.; Liu, Y.F.; Jiang, Y.X. Experimental and numerical study on vibration and structure-borne noise of high-speed railway composite bridge. *Appl. Acoust.* **2022**, *192*, 108757. [CrossRef]
14. He, W.; He, K.; Zou, C.; Yu, Y. Experimental noise and vibration characteristics of elevated urban rail transit considering the effect of track structures and noise barriers. *Environ. Sci. Pollut. Res.* **2021**, *33*, 45903–45919. [CrossRef] [PubMed]
15. Shang, T.; Zhong, H.; Xiao, S.H.; Kong, Y.S. Measurement and analysis of wheel-rail noise in long-span bridges of urban rail transit systems. *Urban. Rail Transit.* **2024**, *37*, 117–124.
16. Chen, Z.; Yang, G.; Ning, J.; Chen, Z.; Yang, J.; Wang, K.; Zhai, W. Dynamic test and analysis of rack vehicle-track coupled system on large slope line. *Meas.* **2024**, *238*, 115263. [CrossRef]
17. Xie, J.; Zhai, W.; Hua, Y. A prediction method for railway-induced vibrations in building structures using modal properties in limited modes. *J. Build. Eng.* **2024**, *95*, 110120. [CrossRef]
18. Sheng, X.Z.; Cheng, G.; Thompson, D.J.; Ge, S. Research progress of wheel-rail noise prediction model. *J. Transp. Eng.* **2021**, *21*, 20–38.
19. Zhang, X.; Li, X.; Li, X.; Liu, Q.; Zhang, Z. Train-induced vibration and noise radiation of a prestressed concrete box-girder. *Noise Control Eng. J.* **2013**, *61*, 425–435. [CrossRef]
20. Li, Q.; Song, X.; Wu, D. A 2.5-dimensional method for the prediction of structure borne low-frequency noise from concrete rail transit bridges. *J. Acoust. Soc. Am.* **2014**, *135*, 2718–2726. [CrossRef]
21. Song, X.D.; Wu, D.J.; Li, Q.; Botteldooren, D. Structure-borne low-frequency noise from multi-span bridges: A prediction method and spatial distribution. *J. Sound Vib.* **2016**, *367*, 114–128. [CrossRef]
22. Song, X.D.; Li, Q.; Wu, D.J. Investigation of rail noise and bridge noise using a combined 3D dynamic model and 2.5D acoustic model. *Appl. Acoust.* **2016**, *109*, 5–17. [CrossRef]
23. Song, L.; Li, X.; Zheng, J.; Guo, M.; Wang, X. Vibro-acoustic analysis of a rail transit continuous rigid frame box girder bridge based on a hybrid WFE-2D BE method. *Appl. Acoust.* **2020**, *157*, 107028. [CrossRef]
24. Yu, L.; Lei, X.; Luo, K. Noise analysis of box girder structure based on hybrid finite element-statistical energy analysis. *J. Appl. Acoust.* **2021**, *40*, 163–172.
25. Liu, X.; Zhang, N.; Sun, G. Vibration and noise prediction and experimental verification of steel-concrete composite box girder bridge for high-speed railway. *China Civ. Eng. J.* **2023**, *56*, 41–50.
26. *HJ 2.4-2021*; Technical Guidelines for Noise Impact Assessment. Ministry of Ecology and Environment: Beijing, China, 2021.
27. Ozkurt, N.; Sari, D.; Akdag, A.; Kutukoglu, M.; Gurarslan, A. Modeling of noise pollution and estimated human exposure around Istanbul Atatürk Airport in Turkey. *Sci. Total Environ.* **2014**, *482–483*, 486–492. [CrossRef]
28. Mann, S.; Singh, G. Traffic noise monitoring and modelling-an overview. *Environ. Sci. Pollut. Res.* **2022**, *29*, 55568–55579. [CrossRef]
29. Tezel-Oguz, M.N.; Marasli, M.; Sari, D.; Ozkurt, N.; Keskin, S.S. Investigation of simultaneous effects of noise barriers on near-road noise and air pollutants. *Sci. Total Environ.* **2023**, *892*, 164754. [CrossRef]

30. Kwon, H.-W.; Hong, S.-Y.; Song, J.-H. Development of a noise prediction software NASEFA and its application in medium-to-high frequency ranges. *Adv. Eng. Softw.* **2015**, *83*, 213–216. [CrossRef]
31. Constantinou, E.; Kakarontzas, G.; Stamelos, I. An automated approach for noise identification to assist software architecture recovery techniques. *J. Syst. Softw.* **2015**, *107*, 118–122. [CrossRef]
32. Bravo-Moncayo, L.; Lucio-Naranjo, J.; Chávez, M.; Pavón-García, I.; Garzón, C. A machine learning approach for traffic-noise annoyance assessment. *Appl. Acoust.* **2019**, *156*, 262–270. [CrossRef]
33. Tiwari, S.K.; Kumaraswamidhas, L.A.; Patel, R.; Garg, N.; Vallisree, S. Traffic noise measurement, mapping, and modeling using soft computing techniques for mid-sized smart Indian city. *Sensors* **2024**, *33*, 101203. [CrossRef]
34. Yang, X.; Han, Z.; Lu, X.; Zhang, Y. A rapid approach to urban traffic noise mapping with a generative adversarial network. *Appl. Acoust.* **2025**, *228*, 110268. [CrossRef]
35. *HJ453-2018*; Technical Guidelines for Environmental Impact Assessment—Urban Rail Transit. Ministry of Ecology and Environment: Beijing, China, 2021.
36. Liu, L.-Y.; Song, L.-Z.; Qin, J.-L.; Liu, Q.-M. Review on structure-borne noise of rail transit bridges. *J. Traffic Transp. Eng.* **2021**, *21*, 1–19.
37. *GB3096-2008*; Environmental Quality Standard for Noise. Ministry of Environmental Protection: Beijing, China, 2008.
38. *ISO 9613-2:1996*; Acoustics—Attenuation of Sound during Propagation Outdoors—Part 2: General Method of Calculation. International Organization for Standardization: Geneva, Switzerland, 1996.